Drug Metab. Pharmacokinet. 22 (2): 103-112 (2007).

Regular Article

Morphine Glucuronosyltransferase Activity in Human Liver Microsomes is Inhibited by a Variety of Drugs that are Co-administered with Morphine

Yusuke HARA[1,2], Miki NAKAJIMA[1], Ken-ichi MIYAMOTO[2] and Tsuyoshi YOKOI[1,*]

[1]*Drug Metabolism and Toxicology, Division of Pharmaceutical Sciences, Graduate School of Medical Science, Kanazawa University, Kanazawa, Japan*
[2]*Kanazawa University Hospital, Kanazawa, Japan*

Full text of this paper is available at http://www.jstage.jst.go.jp/browse/dmpk

Summary: Morphine is an analgesic drug used for the treatment of acute and chronic pain syndromes for cancer patients. Glucuronidation is a major pathway of the elimination of morphine in humans. Morphine is metabolized to 3-glucuronide (no analgesic effect) and 6-glucuronide (more potently analgesic than morphine) mainly by UGT2B7. In the present study, we investigated the inhibitory effects of a variety of drugs on the morphine glucuronosyltransferase activities in human liver microsomes. Twenty-one drugs including anticancer drugs, immunosuppresants, analgesics, anticonvulsants, antidepressants, antipsychotic drugs were selected in this study, because they are frequently co-administered with morphine. We found that 10 out of 21 drugs, tamoxifen, tacrolimus, diclofenac, carbamazepine, imipramine, clomipramine, amitriptyline, diazepam, lorazepam and oxazepam extensively inhibited the morphine 3- and 6-glucuronosyltransferase activities. Although some of the drugs are not substrates of UGT2B7, they would be potent inhibitors of UGT2B7. If patients receive morphine and these drugs simultaneously, the drug-drug interaction may change the levels of morphine and these glucuronides, resulting in altered analgesic efficacy and the risk of side effects. The results presented here will assist clinicians in choosing the proper drugs and/or dosages, and enable them to anticipate potential drug-drug interactions.

Key words: UDP-glucuronosyltrasnferase; glucuronidation; drug-dug interaction; morphine

Introduction

Morphine is an analgesic drug used for the treatment of acute and chronic pain syndromes. It is used as the most practical and versatile analgesic for the relief of severe pain associated with advanced cancer in palliative care.[1)] Morphine is extensively glucuronidated, and this pathway accounts for approximately two-thirds of the elimination of morphine in humans. Morphine is metabolized to morphine 3- and 6-glucuronides by UDP-glucuronosyltransferases (UGTs) in liver.[2,3)] Morphine 3-glucuronidation is the dominant pathway. The metabolic clearance to morphine 3-glucuronide is about 5-fold higher than the metabolic clearance to morphine 6-glucuronide.[4)] Morphine 3-glucuronide has no analgesic effects, but morphine 6-glucuronide is a more potent (20 times) analgesic than morphine itself.[5)]

Patients suffering from cancer need continuous therapy with morphine. Anti-cancer drugs such as etoposide, irinotecan (its active metabolite is SN-38), and tamoxifen, are widely used for chemotherapy with morphine. Immunosuppressant drugs such as tacrolimus, cyclosporine A, and mycophenolate are sometimes used with morphine for the treatment of pain after organ transplantation. Cancer patients may also receive analgesics (diclofenac, acetaminophen, and naloxone), anticonvulsants (carbamazepine and valproic acid), and antidepressants (imipramine, clomipramine, amitriptyline, and desipramine) for the treatment of neuropathic pain from cancer. In addition, 10-30% of cancer patients have psychological distress.[6,7)] For the treatment of the psychological distress, benzodiazepine agonists (diazepam, lorazepam and oxazepam) and antipsychorotic drugs (olanzapine and milnacipran) are

Received; November 10, 2006, Accepted; February 1, 2007
**To whom correspondence should be addressed*: Tsuyoshi YOKOI, Ph.D., *Drug Metabolism and Toxicology, Division of Pharmaceutical Sciences, Graduate School of Medical Science, Kanazawa University, Kakuma-machi, Kanazawa 920-1192, Japan. Tel. & Fax. ~81-76-234-4407, E-mail: TYOKOI • kenroku.kanazawa-u.ac.jp*

used. Thus, morphine is frequently co-administered with a variety of drugs. Since the clearance of morphine is dependent on the metabolism by UGTs, drugs that inhibit UGTs might affect the kinetics of morphine and its glucuronides, resulting in altered analgesic efficacy and the risk of side effects. In the present study, we investigated the inhibitory effects of a variety of drugs that are frequently co-administered with morphine, on morphine glucuronidation in human livers in order to obtain useful information for predicting drug-drug interactions.

Materials and Methods

Chemicals and reagents: Morphine hydrochloride was purchased from Takeda Chemical Industries (Osaka, Japan). Morphine 3- and 6-glucuronides were generous gifts from Dr. Kazuta Oguri, Kyushu University (Fukuoka, Japan). Etoposide, tamoxifen citrate, cyclosporine A, mycophenolate, acetaminophen, valproic acid, carbamazepine, imipramine hydrochloride, clomipramine hydrochloride, amitriptyline hydrochloride, desipramine hydrochloride, diazepam, lorazepam, oxazepam were purchased from Wako Pure Chemical Industries (Osaka, Japan). Diclofenac, naloxone, uridine 5′-diphosphoglucronic acid (UDPGA), and alamethicin were purchased from Sigma-Aldrich (St. Louis, MO). Tacrolimus was purchased from Calbiochem (La Jolla, CA). Olanzapine was from Toronto Research Chemicals (Toronto, Canada). Irinotecan and SN-38 were kindly provided by Yakult (Tokyo, Japan). Milnacipran hydrochloride was kindly provided by Asahikasei Pharma (Tokyo, Japan). Pooled human liver microsomes were obtained from BD Gentest (Woburn, MA). All other chemicals were of the highest grade commercially available.

Morphine glucuronosyltransferase activity: Morphine glucuronosyltransferase activity was determined as described previously[8] with slight modifications. A typical incubation mixture (0.2 mL total volume) contained 50 mM Tris-HCl buffer (pH 7.4), 5 mM $MgCl_2$, 5 mM UDPGA, 25 μg/mL alamethicin, 0.25 mg/mL microsomal protein and 25–200 μM morphine. Each drug, which was dissolved in methanol, was added as an inhibitor so that the final concentration of solvent in the incubation mixture was $<1\%$. The reaction was initiated by the addition of UDPGA. After incubation at 37°C for 30 min, the reaction was terminated by the addition of 0.1 mL of ice-cold perchloric acid. After the removal of protein by centrifugation at 10,000 *g* for 5 min, a 100 μL portion of the supernatant was subjected to HPLC. Chromatography was performed using an L-2130 pump (Hitachi, Tokyo, Japan), an L-2480 FL detector (Hitachi), an L-2200 autosampler (Hitachi), a D-2500 integrator (Hitachi), and an L-2300 column oven (Hitachi). The flow rate was 0.8 mL/min and the column temperature was 35°C. The glucuronides were detected fluorometrically (excitation: 210 nm; emission: 350 nm) with a noise-base clean Uni-3 (Union, Gunma, Japan). The analytical column was a Develosil C30 (4.6 § 150 mm; 5 μm) column (Nomura Chemical, Aichi, Japan) and the mobile phase was 50 mM sodium dihydrogen phosphate (pH 4.5). The retention times of morphine 3-glucuronide, morphine 6-glucuronide, and morphine were 18.5, 31.0 and 37.5 min, respectively. The quantification of the metabolites was performed by comparing the HPLC peak heights to those of authentic standards. Limits of detection of morphine 3- and 6-glucuronides were 20 fmol and 200 fmol, respectively. It was also confirmed that intra-day and inter-day precision and accuracy of the detection of the glucuronides were $<10\%$ (data not shown). The formation of morphine 3- and 6-glucuronides by human liver microsomes increased linearly with an incubation time up to 60 min and with a protein concentration up to 0.75 mg/mL. Unless specified, an incubation time of 30 min and 0.25 mg/mL microsomal protein were used. All data were analyzed using the mean of duplicate determinations. The variances between the duplicate determinations were $<10\%$.

Data analyses: Lineweaver-Burk plots were used for the determination of the type of inhibition,[9] and Dixon plots were used as a secondary method. Kinetic parameters were determined by a nonlinear regression analysis using a computer program (K-cat, BioMetallics, Princeton, NJ).

Prediction of *in vivo* drug-drug interactions from *in vitro* data: If an enzyme reaction is inhibited competitively or noncompetitively by other drugs, when the substrate concentration is much lower than K_m, the change in the intrinsic clearance (CL_{int}) is expressed by the following equation[10]:

$$CL_{int}(\sim\text{inhibitor})/CL_{int}(\ \text{inhibitor})\quad 1/(1\sim I/K_i)$$

where I is the concentration of the inhibitor and K_i is the inhibition constant. When we discuss drug-drug interactions *via* the inhibition of enzymes, it is important that the concentration of the inhibitor refers to the concentration of the drug around the enzyme. It is difficult to know the actual concentrations of drugs at the active site of UGT. The changes of CL_{int} caused by co-administered drugs can be predicted using the maximum unbound concentrations in the liver. Since data of the concentrations in the liver and protein binding of each drug in tissues are largely not available, the maximum plasma concentrations were alternatively used in the present study.

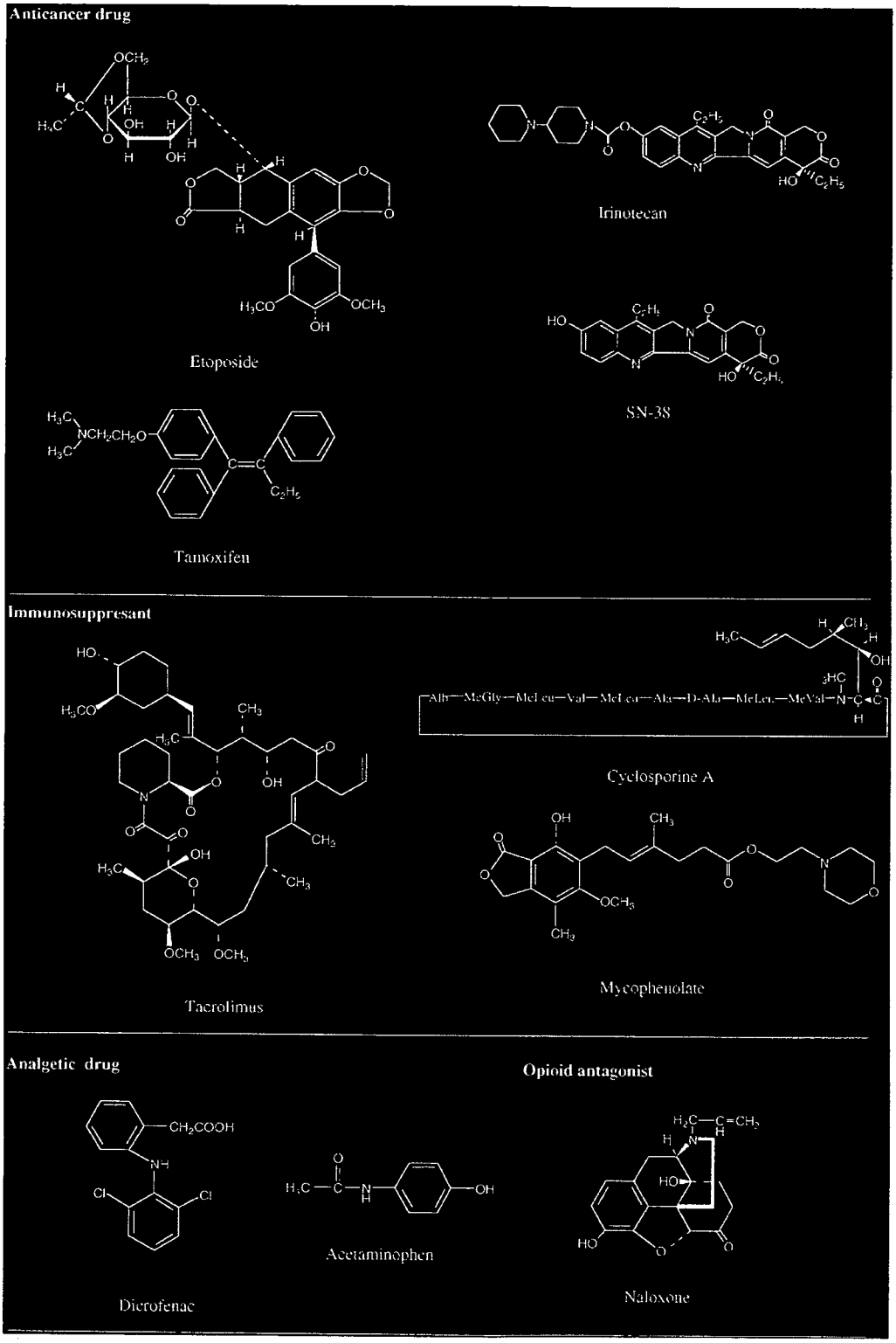

Fig. 1. Structure of drugs used in the present study.

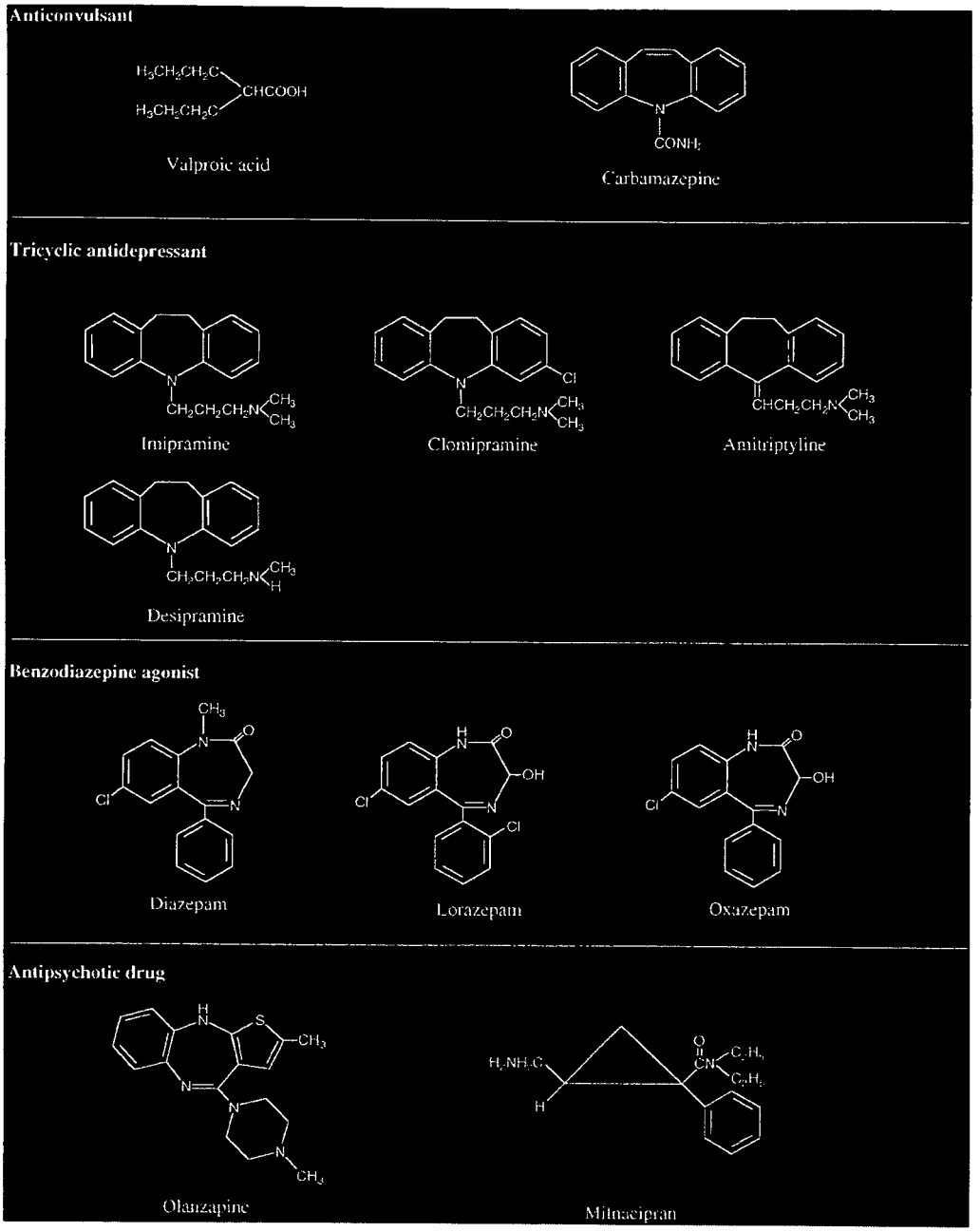

Fig. 1. Continued

Results

Inhibitory effects of drugs on morphine glucuronosyltransferase activities in human liver microsomes: Twenty-one drugs (500 μM) were screened for the inhibitory effects on morphine 3- and 6-glucuronosyltransferase activities at a 50 μM substrate concentration. As shown in **Fig. 2**, the morphine 3- and 6-glucuronosyltransferase activities were strongly inhibited by tamoxifen, diclofenac, imipramine, clomipramine, amitriptyline, desipramine, diazepam, lorazepam and oxazepam (<20% of control). The activities were also moderately inhibited by tacrolimus, mycophenolate, naloxone, carbamazepine, and olanzapine (20–50% of control), and weakly inhibited by irinotecan and valproic acid (50–70% of control). Interestingly, the morphine glucuronosyltransferase activities were activated by cyclosporine A (120%). For 14 drugs showing >50% inhibition at 500 μM, the IC_{50} values were determined by dose response curves with various

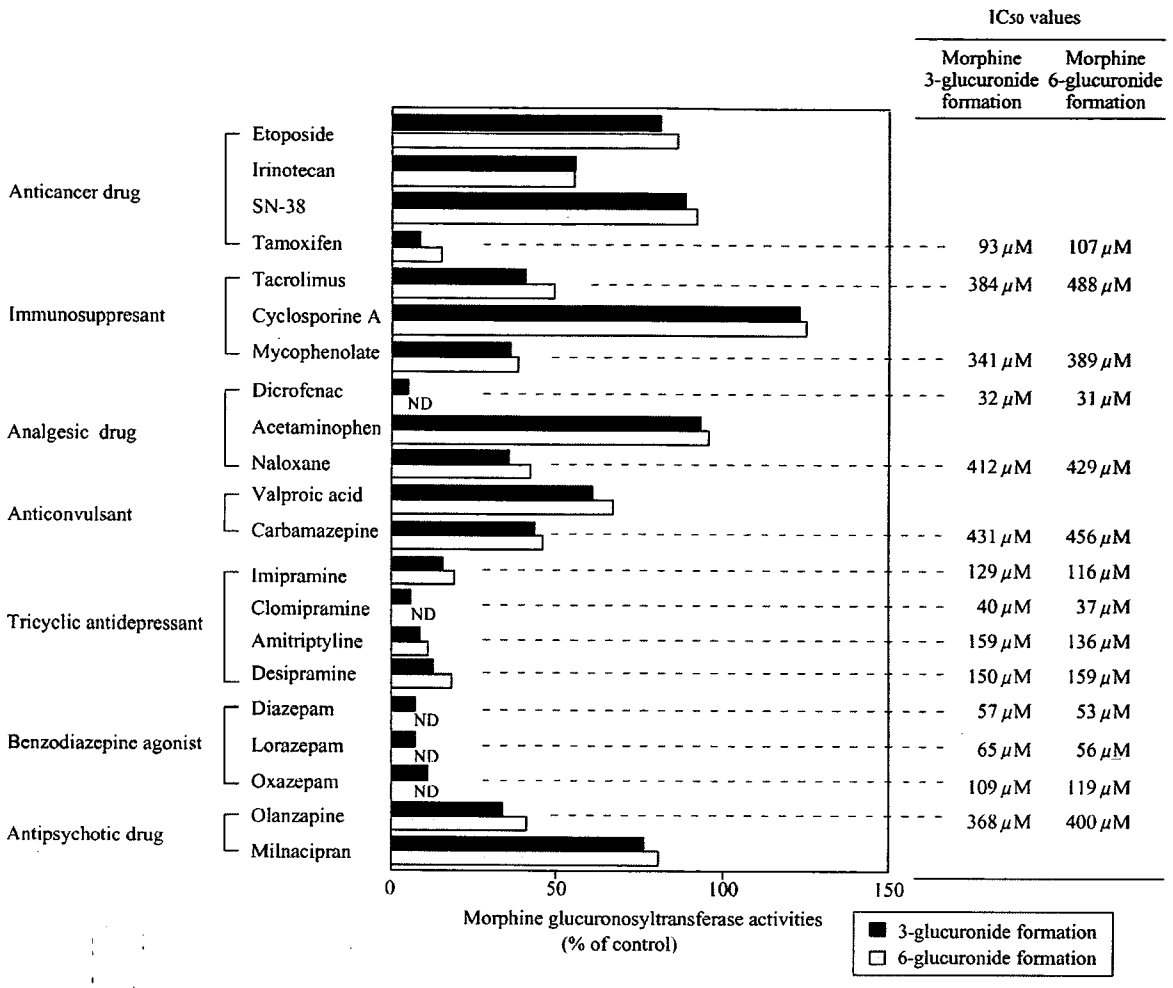

Fig. 2. Inhibitory effects of drugs on morphine glucuronosyltransferase activities in human liver microsomes. The concentrations of morphine and each drug were 50 μM and 500 μM, respectively. Each column represents the mean of duplicate determinations. The control activities in the pooled human liver microsomes were 23.1 pmol/min/mg protein for morphine 3-glucuronosyltransferase activity and 5.4 pmol/min/mg protein for morphine 6-glucuronosyltransferase activity. ND, not detected.

concentrations. The IC_{50} values are summarized in **Fig. 2.** The IC_{50} values of each drug were similar between the morphine 3- and 6-glucuronosyltransferase activities.

Inhibition constant and inhibition pattern: We determined the inhibition constant (K_i) values for 14 drugs that inhibited the morphine glucuronosyltransferase activities (IC_{50} values were $<500\,\mu$M), **(Fig. 3 and Table 1).** The K_{is} and K_{ii} values are inhibition constants on the slope (competitive) and on the intercept (noncompetitive), respectively. Tamoxifen, mycophenolate, diclofenac, diazepam, and olanzapine exhibited noncompetitive inhibition for both the morphine 3- and 6-glucuronosyltransferase activities. Tacrolimus, carbamazepine, and lorazepam exhibited a mixed type of competitive and noncompetitive inhibition for both activities. Naloxone, imipramine, clomipramine, amitriptyline, and desipramine exhibited noncompetitive and mixed type inhibitions for morphine 3- and 6-glucuronosyltransferase activities, respectively. Oxazepam exhibited competitive and mixed type inhibitions for morphine 3- and 6-glucuronosyltransferase activities, respectively. All compounds except naloxone and olanzapine more potently inhibited the morphine 6-glucuronosyltransferase activity than the morphine 3-glucuronosyltransferase activity.

Predicted change of *in vivo* clearance of morphine by a variety of drugs from *vitro* data: To predict the possibility of drug-drug interaction *via* a metabolic process between morphine and the 14 drugs, the $1\sim I/K_i$ values were calculated **(Table 1).** Carbamazepine showed the highest $1\sim I/K_i$ values (1.4 and 1.9 for morphine 3- and 6-glucuronosyltransferase activities, respectively). The values by diclofenac were both 1.4 for morphine 3- and 6-glucuronosyltransferase activities. Mycophenolate, clomipramine, diazepam and

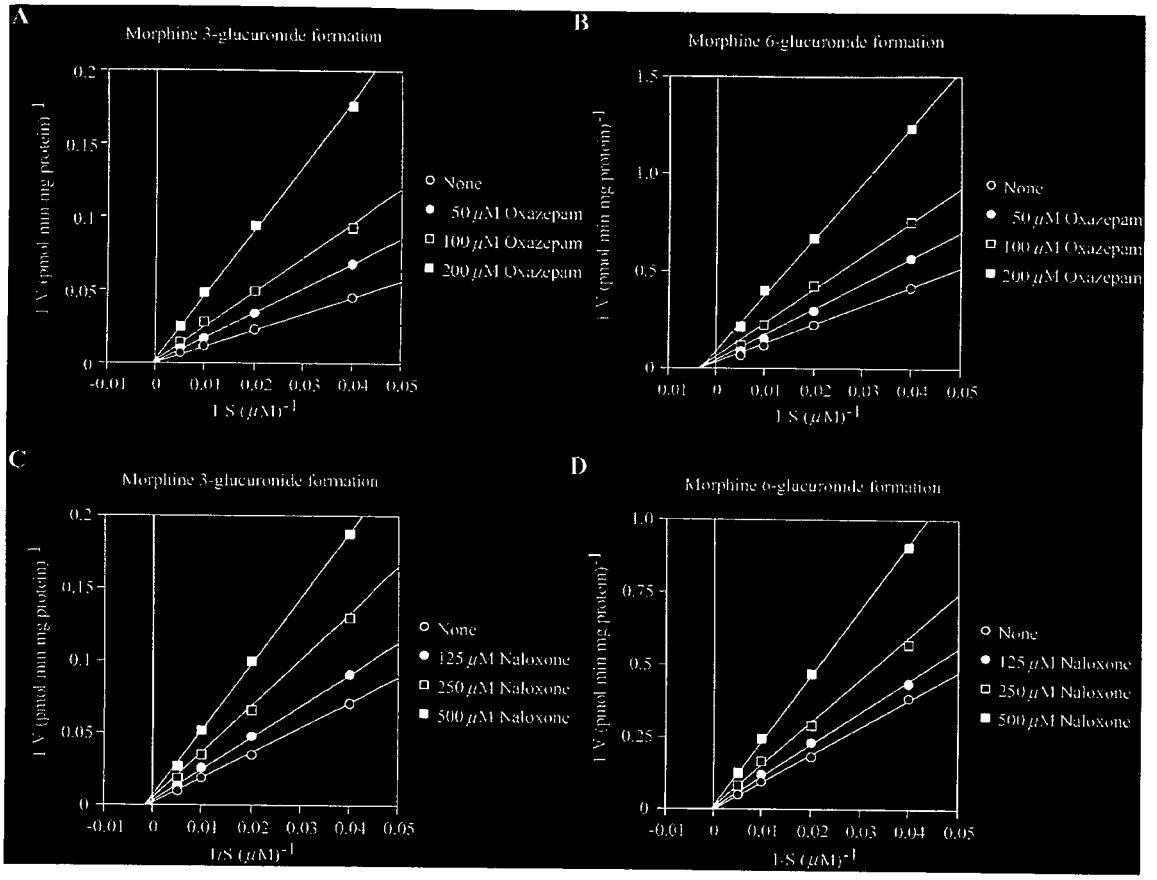

Fig. 3. Typical Lineweaver-Burk plots of morphine glucuronosyltransferase activities in human liver microsomes. Effects of oxazepam (A, B) or naloxone (C, D) on morphine 3-(A, C) and 6-(B, D) glucuronosyltransferase activities were investigated. Each data point represents the mean of duplicate determinations. Lines were drawn by linear regression analysis.

Table 1. Inhibition of morphine 3- and 6-glucuronosyltransferase activity in human liver microsomes by 14 drugs.

Drug	I (μM)	Morphine 3-glucuronosyltransferase activity				Morphine 6-glucuronosyltransferase activity			
		K_{is} (μM)	K_{ii} (μM)	Inhibitory type	1~I/K_i	K_{is} (μM)	K_{ii} (μM)	Inhibitory type	1~I/K_i
Tamoxifen	0.48		81	Noncompetitive	1.0		27	Noncompetitive	1.0
Tacrolimus	0.04	347	95	Mixed	1.0	101	46	Mixed	1.0
Mycophenolate	60		713	Noncompetitive	1.1		296	Noncompetitive	1.2
Diclofenac	9.4		22	Noncompetitive	1.4		24	Noncompetitive	1.4
Naloxone	0.05		518	Noncompetitive	1.0	1298		Competitive	1.0
Carbamazepine	42	243	118	Mixed	1.4	78	47	Mixed	1.9
Imipramine	1.9		81	Noncompetitive	1.0	60	33	Mixed	1.1
Clomipramine	1.4		20	Noncompetitive	1.1	19	6	Mixed	1.2
Amitriptyline	0.8		248	Noncompetitive	1.0	111	30	Mixed	1.0
Desipramine	1.1		177	Noncompetitive	1.0	458	111	Mixed	1.0
Diazepam	1.8		47	Noncompetitive	1.0		9	Noncompetitive	1.2
Lorazepam	0.2	239	53	Mixed	1.0	65	17	Mixed	1.0
Oxazepam	5	519		Competitive	1.0	41	93	Mixed	1.2
Olanzapine	0.04		196	Noncompetitive	1.0		266	Noncompetitive	1.0

The K_{is} and K_{ii} values are inhibition constants on the slope (competitive) and on the intercept (noncompetitive), respectively.
In the case of mix-type inhibition, the lower K_i was used in the calculation.
The plasma concentration of oxazepam was from Court *et al.*,[19] and those of the other drugs were from Gilman *et al.*[24]

oxazepam showed the $1\sim I/K_i$ values of 1.2 for the morphine 6-glucuronosyltransferase activity. Since most compounds more potently inhibit morphine 6-glucuronosyltransferase activity than morphine 3-glucuronosyltransferase activity, the ratio of 3-glucuronide/6-glucuronide in plasma would be increased, changing the analgesic efficacy and the risk of side effects.

Discussion

Morphine is mainly metabolized to 3- and 6-glucuronides by UGT enzymes. Morphine 3-glucuronidation is catalyzed by multiple isoforms such as UGT2B7, UGT1A8, and UGT1A3 with relatively low K_m values (0.4–3.2 mM) as well as UGT1A10, UGT1A6, UGT1A1, and UGT1A9 with relatively high K_m values (13–37 mM).[3] In contrast, morphine 6-glucuronidation is specifically catalyzed by UGT2B7 (K_m 1.0 mM).[3] Collectively. UGT2B7 is recognized as a major isoform catalyzing the glucuronidation of morphine. In the presents study, we investigated the inhibitory effects of 21 drugs on the morphine glucuronosyltransferase activities. Although the K_m values of the morphine glucuronosyltransferase activities are high as mM order, the inhibitory effects were investigated with the substrate concentrations at μM order by considering the plasma concentrations in clinical practice[11] and the detection limits of morphine glucuronides in the HPLC system.

Among 21 drugs used in the present study, diclofenac, clomipramine, and amitriptyline have been reported to affect the pharmacokinetics of morphine *in vivo*. Tighe *et al.*[11] have reported that the plasma concentration of morphine 6-glucuronide was decreased by 40% with co-administration of diclofenac. Diclofenac is known to be mainly metabolized by P450s, but also metabolized by UGTs (**Table 2**). The affinity of diclofenac to UGT2B7 (K_m 25 μM) is higher than that of morphine.[12] In the present study, we found that diclofenac potently inhibited the morphine glucuronosyltransferase activities in a noncompetitive manner. The extent of *in vivo* inhibition can be predicted quantitatively by the calculation of $1/(1\sim I/K_i)$ from an *in vitro* study. The $1\sim I/K_i$ values by diclofenac were 1.4, indicating that the change of the plasma concentration would be due to the inhibition of morphine glucuronidation by diclofenac. Ventafridda *et al.*[13] reported that co-administration of clomipramine and amitriptyline increased the area under the curve (AUC) of morphine approximately 2 fold in humans. Tricyclic antidepressants including clomipramine and amitriptyline are known to be substrates of UGT1A3 and UGT1A4 (**Table 2**). However, we found that clomipramine (K_i values were 6–20 μM) and amitriptyline (K_i values were 30–248 μM) strongly inhibited the morphine glucuronidations. These results are in accordance with a previous study by Wahlstrom *et al.*[14] reporting that clomipramine (K_i values were 56–90 μM) and amitriptyline (K_i values were 80–160 μM) inhibited morphine glucuronidations in human liver microsomes. The $1\sim I/K_i$ values by clomipramine were at most 1.2, but those by amitriptyline were 1.0, indicating that the prediction of *in vivo* inhibition from *in vitro* data might be unsuccessful. For drugs that are cleared predominantly through CYP-mediated metabolism, there is growing evidence that successful prediction of *in vivo* drug interactions through the inhibition of metabolism can be made from *in vitro* data. In contrast, drugs that are mainly metabolized by UGT appear to be

Table 2. Drugs used in this study and the involvement of UGTs in their metabolism.

Drug	UGT isoforms	K_m (μM)	Excretion as glucuronide
Etoposide	UGT1A1[25]	503	15–30%[26]
Irinotecan	UGT1A1[27]	unknown	unknown
SN-38	UGT1A1[28]	24	14.7%[29]
	UGT1A4	147	
	UGT1A6	97	
	UGT1A9	13	
	UGT2B15	186	
Tamoxifen	UGT1A4[21]	32	unknown
Tacrolimus	UGT2B7[30]	449	unknown
Cyclosporine	UGT2B7[31]	202	unknown
Mycophenolate	UGT1A1[9]	185	96%[32]
	UGT1A7	30	
	UGT1A8	298	
	UGT1A9	291	
	UGT1A10	119	
Diclofenac	UGT1A3[12]	12	5–10%[33]
	UGT2B7	25	
Acetaminophen	UGT1A1[34]	9400	63%[35]
	UGT1A6	2200	
	UGT1A9	20900	
Naloxone	UGT1A3[36]	unknown	unknown
	UGT2B7	unknown	
Carbamazepine	UGT2B7[15]	214	15%[37]
Valproic acid	UGT1A6[38]	3200	10%[39]
	UGT1A9	5200	
	UGT2B7	2100	
Imipramine	UGT1A3[40]	472	0.1–0.8%[41]
	UGT1A4	310	
Clomipramine	UGT1A3[40]	unknown	0.1–0.8%[41]
	UGT1A4	unknown	
Amitriptyline	UGT1A3[40]	267	26%[42]
	UGT1A4	170	
Desipramine	UGT1A3[40]	unknown	0.1–0.8%[41]
	UGT1A4	unknown	
Diazepam	unknown	unknown	unknown
Lorazepam	UGT2B7[18]	unknown	86%[43]
	UGT2B15[19]	unknown	
Oxazepam	UGT2B7[18]	203	67%[45]
	UGT2B15[44]	32	
Olanzapine	UGT1A4[46]	227	25%[47]
Milnacipran	unknown	unknown	30%[48]

less well-predicted using *in vitro* data. This may be due to the nature of UGT, latency restricting the access of substrates or UDPGA and the removal of formed glucuronide. Thus, for drugs that are mainly metabolized by UGT, the calculation of $1\sim I/K_i$ may not necessarily give a plausible prediction. We found that imipramine and desipramine also prominently inhibited the morphine glucuronosyltransferase activities. Although the $1\sim I/K_i$ was at most 1.1, it might be necessary to pay attention to the co-administration of these tricyclic antidepressants with morphine.

By calculation of the $1\sim I/K_i$ value, it was predicted that carbamazepine might cause drug-drug interactions with morphine. Carbamazepine is mainly metabolized by P450s, but also glucuronidated by UGT2B7 (**Table 2**).[15] The affinity of carbamazepine to UGT2B7 (K_m 214 μM) is higher than that of morphine.[15] Although the contribution of UGT to carbamazepine metabolism might be low, our data suggest that the co-administration of carbamazepine and morphine should be avoided in clinical practice.

We found that benzodiazepine agonists have inhibitory effects on the morphine glucuronosyltransferase activities. The order of inhibitory potencies was diazepam > lorazepam > oxazepam. The results were consistent with a previous report that these drugs inhibit zidovudine glucuronosyltransferase activity catalyzed by UGT2B7 in human liver microsomes.[16,17] Lorazepam and oxazepam are mainly metabolized by UGT2B7 and 2B15,[18,19] whereas diazepam is mainly metabolized to oxazepam by CYPs.[20] It is clearly demonstrated that these drugs are potent inhibitors of UGT2B7. Co-administration of these benzodiazepine agonists with morphine should also be avoided.

Tamoxifen and tacrolimus strongly inhibited the morphine glucuronosyltransferase activities. Although tamoxifen has been reported to be a substrate of UGT1A4,[21] it is a potent inhibitor of UGT2B7 (K_i values were 27–81 μM), like tricyclic antidepressants. Tacrolimus, which is a substrate of UGT2B7, inhibited morphine glucuronosyltransferase activities with a mixed type of competitive and noncompetitive inhibition (K_i values were 46–347 μM). A drug-drug interaction between morphine and tamoxifen or tacrolimus might be possible.

Recently, it was reported that ketoconazole, which is a well-known inhibitor of CYP3A4, potently inhibits the morphine glucuronosyltransferase activity catalyzed by recombinant UGT2B7 (K_i values were 110–120 μM).[22] The possibility has been suggested that CYPs may interact with UGTs to modulate the function of UGTs.[23] The drugs showing potent inhibitory effects on morphine glucuronidation (**Table 1**) were substrates of CYPs (clomipramine, amitriptyline, tamoxifen: CYP2D6, diclofenac: CYP2C9, diazepam, lorazepam: CYP3A4). It would be interesting to investigate whether possible interaction between these CYP isoforms and UGT2B7 might be related to the inhibitory effects.

In conclusion, we found that tamoxifen, tacrolimus, diclofenac, carbamazepine, imipramine, clomipramine, amitriptyline, diazepam, lorazepam and oxazepam have prominent inhibitory effects on morphine glucuronidation. If patients receive morphine and these drugs simultaneously, drug-drug interactions may result in changed analgesic efficacy and risk of side effects. Such understanding is important so that clinicians can choose the proper drugs and/or dosages, and anticipate potential drug-drug interactions.

Acknowledgement: We acknowledge Brent Bell for reviewing the manuscript.

This work was supported in part by the Grant-in-Aid for Cancer Research (17-8) from the Ministry of Health, Labor and Welfare of Japan.

References

1) Donnelly, S., Davis, M. P., Walsh, D. and Naughton, M.: Morphine in cancer pain management: a practical guide. *Support Care Cancer*, **10**: 13–35 (2002).
2) Coffman, B. L., Rios, G. R., King, C. D. and Tephly, T. R.: Human UGT2B7 catalyzes morphine glucuronidation. *Drug Metab. Dispos.*, **25**: 1–4 (1997).
3) Stone, A. N., Mackenzie, P. I., Galetin, A., Houston, J. B. and Miners, J. O.: Isoform selectivity and kinetics of morphine 3- and 6-glucuronidation by human UDP-glucuronosyltransferases: evidence for atypical glucuronidation kinetics by UGT2B7. *Drug Metab. Dispos.*, **31**: 1086–1089 (2003).
4) Milne, R. W., Nation, R. L. and Somogyi, A. A.: The disposition of morphine and its 3- and 6-glucuronide metabolites in humans and animals, and the importance of the metabolites to the pharmacological effects of morphine. *Drug Metab. Rev.*, **28**: 345–472 (1996).
5) Lotsch, J., Skarke, C., Tegeder, I. and Geisslinger, G.: Drug interactions with patient-controlled analgesia. *Clin. Pharmacokinet.*, **41**: 31–57 (2002).
6) Akechi, T., Okamura, H., Nishiwaki, Y. and Uchitomi, Y.: Psychiatric disorders and associated and predictive factors in patients with unresectable non small cell lung carcinoma: a longitudinal study. *Cancer*, **92**: 2609–2622 (2001).
7) Uchitomi, Y., Mikami, I., Nagai, K., Nishiwaki, Y., Akechi, T. and Okamura, H.: Depression and psychological distress in patients during the year after curative resection of non-small-cell lung cancer. *J. Clin. Oncol.*, **21**: 69–77 (2003).
8) Milne, R. W., Nation, R. L., Reynolds, G. D., Somogyi, A. A. and Van Crugten, J. T.: High-performance liquid chromatographic determination of morphine and its 3- and 6-glucuronide metabolites: improvements to the method and application to stability studies. *J. Chromatogr.*, **565**: 457–464 (1991).
9) Segel, I. H.: Rapid equilibrium partial and mixed type

inhibition. *In. Enzyme. Kinetics*, A Wiley-Interscience Publication, New York, 2004, pp. 161–226.
10) Ito, K., Iwatsubo, T., Kanamitsu, S., Ueda, K., Suzuki, H. and Sugiyama, Y.: Prediction of pharmacokinetic alteration caused by drug-drug Interactions: Metabolic interaction in the liver. *Pharmacol. Rev.*, **50**: 387–411 (1998).
11) Tighe, K. E., Webb, A. M. and Hobbs, G. J.: Persistently high plasma morphine-6-glucuronide levels despite decreased hourly patient-controlled analgesia morphine use after single-dose diclofenac: potential for opioid-related toxicity. *Anesth. Analg.*, **88**: 1137–1142 (1999).
12) Sakaguchi, K., Green, M., Stock, N., Reger, T. S., Zunic, J. and King, C.: Glucuronidation of carboxylic acid containing compounds by UDP-glucuronosyltransferase isoforms. *Arch. Biochem. Biophys.*, **424**: 219–225 (2004).
13) Ventafridda, V., Bianchi, M., Ripamonti, C., Sacerdote, P., De Conno, F., Zecca, E. and Panerai, A. E.: Studies on the effects of antidepressant drugs on the antinociceptive action of morphine and on plasma morphine in rat and man. *Pain*, **43**: 155–162 (1990).
14) Wahlstrom, A., Lenhammar, L., Ask, B. and Rane, A.: Tricyclic antidepressants inhibit opioid receptor binding in human brain and hepatic morphine glucuronidation. *Pharmacol. Toxicol.*, **75**: 23–27 (1994).
15) Staines, A. G., Coughtrie, M. W. and Burchell, B.: N-glucuronidation of carbamazepine in human tissues is mediated by UGT2B7. *J. Pharmacol. Exp. Ther.*, **311**: 1131–1137 (2004).
16) Grancharov, K., Naydenova, Z., Lozeva, S. and Golovinsky, E.: Natural and synthetic inhibitors of UDP-glucuronosyltransferase. *Pharmacol. Ther.*, **89**: 171–186 (2001).
17) Barbier, O., Turgeon, D., Girard, C., Green, M. D., Tephly, T. R., Hum, D. W. and Belanger, A.: 3′-azido-3′-deoxythimidine (AZT) is glucuronidated by human UDP-glucuronosyltransferase 2B7 (UGT2B7). *Drug Metab. Dispos.*, **28**: 497–502 (2000).
18) Liston, H. L., Markowitz, J. S. and DeVane, C. L.: Drug glucuronidation in clinical psychopharmacology. *J. Clin. Psychopharmacol.*, **21**: 500–515 (2001).
19) Court, M. H., Duan, S. X., Guillemette, C., Journault, K., Krishnaswamy, S., von Moltke, L. L. and Greenblatt, D. J.: Stereoselective conjugation of oxazepam by human UDP-glucuronosyltransferases (UGTs): *S*-oxazepam is glucuronidated by UGT2B15, while *R*-oxazepam is glucuronidated by UGT2B7 and UGT1A9. *Drug Metab. Dispos.*, **30**: 1257–1265 (2002).
20) Mandelli, M., Tognoni, G. and Garattini, S.: Clinical pharmacokinetics of diazepam. *Clin. Pharmacokinet.*, **3**: 72–91 (1978).
21) Kaku, T., Ogura, K., Nishiyama, T., Ohnuma, T., Muro, K. and Hiratsuka, A.: Quaternary ammonium-linked glucuronidation of tamoxifen by human liver microsomes and UDP-glucuronosyltransferase 1A4. *Biochem. Pharmacol.*, **67**: 2093–2102 (2004).
22) Takeda, S., Kitajima, Y., Ishii, Y., Nishimura, Y., Mackenzie, P. I., Oguri, K. and Yamada, H.: Inhibition of UDP-glucuronosyltransferase 2B7-catalyzed morphine glucuronidation by ketoconazole: dual mechanisms involving a novel noncompetitive mode. *Drug Metab. Dispos.*, **34**: 1277–1282 (2006).
23) Fremont, J. J., Wang, R. W. and King, C. D.: Coimmunoprecipitation of UDP-glucuronosyltransferase isoforms and cytochrome P450 3A4. *Mol. Pharmacol.*, **67**: 260–262 (2005).
24) Gilman, A. G., Joel, G., Hardman, J. G. and Limbird, L. E.: The Pharmaceutical Basis of Therapeutics 10th edition, Macmillan PC, New York, 2001, pp. 1948.
25) Watanabe, Y., Nakajima, M., Ohashi, N., Kume, T. and Yokoi, T.: Glucuronidation of etoposide in human liver microsomes is specifically catalyzed by UDP-glucuronosyltransferase 1A1. *Drug Metab. Dispos.*, **31**: 589–595 (2003).
26) Hande, K. R., Wedlund, P. J., Noone, R. M., Wilkinson, G. R., Greco, F. A. and Wolff, S. N.: Pharmacokinetics of high-dose etoposide (VP-16-213) administered to cancer patients. *Cancer Res.*, **44**: 379–382 (1984).
27) Innocenti, F., Iyer, L. and Ratain, M. J.: Pharmacogenetics of anticancer agents: lessons from amonafide and irinotecan. *Drug Metab. Dispos.*, **29**: 596–600 (2001).
28) Hanioka, N., Ozawa, S., Jinno, H., Ando, M., Saito, Y. and Sawada, J.: Human liver UDP-glucuronosyltransferase isoforms involved in the glucuronidation of 7-ethyl-10-hydroxycamptothecin. *Xenobiotica*, **31**: 687–699 (2001).
29) Slatter, J. G., Schaaf, L. J., Sams, J. P., Feenstra, K. L., Johnson, M. G., Bombardt, P. A., Cathcart, K. S., Verburg, M. T., Pearson, L. K., Compton, L. D., Miller, L. L., Baker, D. S., Pesheck, C. V. and Lord, R. S. III: Pharmacokinetics, metabolism, and excretion of irinotecan (CPT-11) following I.V. infusion of [^{14}C]CPT-11 in cancer patients. *Drug Metab. Dispos.*, **28**: 423–433 (2000).
30) Strassburg, C. P., Barut, A., Obermayer-Straub, P., Li Q, Nguyen, N., Tukey, R. H. and Manns, M. P.: Identification of cyclosporine A and tacrolimus glucuronidation in human liver and the gastrointestinal tract by a differentially expressed UDP-glucuronosyltransferase: UGT2B7. *J. Hepatol.*, **34**: 865–872 (2001).
31) Bernard, O. and Guillemette, C.: The main role of UGT1A9 in the hepatic metabolism of mycophenolic acid and the effects of naturally occurring variants. *Drug Metab. Dispos.*, **32**: 775–758 (2004).
32) Shaw, L. M., Mick, R., Nowak, I., Korecka, M. and Brayman, K. L.: Pharmacokinetics of mycophenolic acid in renal transplant patients with delayed graft function. *J. Clin. Pharmacol.*, **38**: 268–275 (1998).
33) Degen, P. H., Dieterle, W., Schneider, W., Theobald, W. and Sinterhauf, U.: Pharmacokinetics of diclofenac and five metabolites after single doses in healthy volunteers and after repeated doses in patients. *Xenobiotica*, **18**: 1449–1455 (1988).
34) Court, M. H., Duan, S. X., von Moltke, L. L., Greenblatt, D. J., Patten, C. J., Miners, J. O. and Mackenzie, P. I.: Interindividual variability in acetaminophen glucuronidation by human liver

microsomes: identification of relevant acetaminophen UDP-glucuronosyltransferase isoforms. *J. Pharmacol. Exp. Ther.*, **299**: 998–1006 (2001).
35) Ameer, B. and Greenblatt, D. J.: Acetaminophen. *Ann. Intern. Med.*, **87**: 202–209 (1977).
36) de Wildt, S. N., Kearns, G. L., Leeder, J. S. and van den Anker, J. N.: Glucuronidation in humans. Pharmacogenetic and developmental aspects. *Clin. Pharmacokinet.*, **36**: 439–452 (1999).
37) Faigle, J. W. and Feldmann, K. F.: Carbamazepine. In Woodbury, D. M. (ed.): *Antiepileptic Drugs 2nd edition*, Raven Press, New York, 1982, pp. 483–495.
38) Ethell, B. T., Anderson, G. D. and Burchell, B.: The effect of valproic acid on drug and steroid glucuronidation by expressed human UDP-glucuronosyltransferases. *Biochem. Pharmacol.*, **65**: 1441–1449 (2003).
39) Kuhara, T., Hirokata, Y., Yamada, S. and Matsumoto, I.: Metabolism of sodium dipropylacetate in human. *Eur. J. Drug Metab. Pharmacokinet.*, **3**: 171–177 (1978).
40) Green, M. D., King, C. D. Mojarrabi, B., Mackenzie, P. I. and Tephly, T. R.: Glucuronidation of amines and other xenobiotics catalyzed by expressed human UDP-glucuronosyltransferase 1A3. *Drug Metab. Dispos.*, **26**: 507–512 (1998).
41) Luo, H., Hawes, E. M., McKay, G., Korchinski, E. D. and Midha, K. K.: N(+)-glucuronidation of aliphatic tertiary amines in human: antidepressant versus antipsychotic drugs. *Xenobiotica*, **25**: 291–301 (1995).
42) Vandel, B., Sandoz, M., Vandel, S., Allers, G. and Volmat, R.: Biotransformation of amitriptyline in depressive patients: urinary excretion of seven metabolites. *Eur. J. Clin. Pharmacol.*, **22**: 239–245 (1982).
43) Greenblatt, D. J., Schillings, R. T., Kyriakopoulos, A. A., Shader, R. I., Sisenwine, S. F., Knowles, J. A. and Ruelius, H. W.: Clinical pharmacokinetics of lorazepam. I. Absorption and disposition of oral ^{14}C-lorazepam. *Clin. Pharmacol. Ther.*, **20**: 329–341 (1976).
44) Chung, J. Y., Cho, J. Y., Yu, K. S., Kim, J. R., Jung, H. R., Lim, K. S., Jang, I. J. and Shin, S. G.: Effect of the *UGT2B15* genotype on the pharmacokinetics, pharmacodynamics, and drug interactions of intravenous lorazepam in healthy volunteers. *Clin. Pharmacol. Ther.*, **77**: 486–494 (2005).
45) Alvan, G., Siwers, B. and Vessman, J.: Pharmacokinetics of oxazepam in healthy volunteers. *Acta Pharmacol. Toxicol.*, **40** Suppl 1: 40–51 (1977).
46) Linnet, K.: Glucuronidation of olanzapine by cDNA-expressed human UDP-glucuronosyltransferases and human liver microsomes. *Hum. Psychopharmacol.*, **17**: 233–238 (2002).
47) Callaghan, J. T., Bergstrom, R. F., Ptak, L. R. and Beasley, C. M.: Olanzapine. Pharmacokinetic and pharmacodynamic profile. *Clin. Pharmacokinet.*, **37**: 177–193 (1999).
48) Puozzo, C., Lens, S., Reh, C., Michaelis, K., Rosillon, D., Deroubaix, X. and Deprez, D.: Lack of interaction of milnacipran with the cytochrome P450 isoenzymes frequently involved in the metabolism of antidepressants. *Clin. Pharmacokinet.*, **44**: 977–988 (2005).

BIOCHEMICAL PHARMACOLOGY 74 (2007) 488–495

available at www.sciencedirect.com

ScienceDirect

journal homepage: www.elsevier.com/locate/biochempharm

Change of drug excretory pathway by CCl_4-induced liver dysfunction in rat

Hirotoshi Okumura [1], *Miki Katoh* [1], *Keiichi Minami*, *Miki Nakajima*, *Tsuyoshi Yokoi* *

Division of Pharmaceutical Sciences, Graduate School of Medical Science, Kanazawa University, Kakuma-machi, Kanazawa 920-1192, Japan

ARTICLE INFO

Article history:
Received 27 February 2007
Accepted 27 April 2007

Keywords:
Liver dysfunction
CMZ
DNA microarray
Excretion
Transporter

ABSTRACT

Liver dysfunction affects the pharmacokinetics of drugs. The liver plays an important role in drug excretion as well as drug metabolism and pharmacokinetics. In the present study, the relationship between changes in the cefmetazole (CMZ) excretory pathway and the degree of liver dysfunction induced by CCl_4 treatment was investigated. CMZ is mainly excreted as an unchanged form in feces in control rats. Depending on the serum levels of aspartate aminotransferase (AST) and alanine aminotransferase (ALT), urinary CMZ excretion was increased, whereas fecal CMZ excretion was decreased in rat with liver dysfunction. The AUC of CMZ in rats with severe liver dysfunction was approximately 2-fold higher than that in control rats. Since drug transporters could be involved in drug excretion, changes in the expression of representative hepatic drug transporters in liver dysfunction were investigated by rat DNA microarray. Basolateral solute carrier transporters such as Ntcp, Oct1, and Oatp2 were decreased and basolateral ATP-binding cassette transporters such as Mrp3 and Mrp4 were increased by the CCl_4 treatment. On the other hand, canalicular Mrp2 and Bsep were decreased, but Mdr1 was increased. However, the transporter system for CMZ has not been identified yet. In conclusion, we clarified that the fecal and urinary excretory profiles of CMZ were changed clearly depending on the serum AST and ALT levels in liver dysfunction. The changes in the CMZ excretory pathway might be responsible for the changes in the expression of drug transporters.

1. Introduction

Liver is the central organ for the detoxification and excretion of many xenobiotics including drugs. Drug excretion may be affected by liver dysfunction, leading to an alteration in the pharmacokinetics [1]. Investigation of the relationship between excretion and liver dysfunction is important for predicting the pharmacokinetics in patients with liver dysfunction to avoid drug adverse reactions. Since impaired liver function would vary due to the severity of liver disease, the pharmacokinetics may become complicated. The purpose of the present study is to elucidate whether the drug excretion

* *Corresponding author at*: Division of Pharmaceutical Sciences, Graduate School of Medical Science, Kanazawa University, Kakuma-machi, Kanazawa 920-1192, Japan. Tel.: +81 76 234 4407; fax: +81 76 234 4407.
E-mail address: TYOKOI@kenroku.kanazawa-u.ac.jp (T. Yokoi).

[1] These two authors equally contributed to this work.

Abbreviations: ABC, ATP-binding cassette; ALT, alanine aminotransferase; AST, aspartate aminotransferase; AUC, area under the serum concentration–time curve; Bcrp, breast cancer resistance protein; Bsep, bile-salt export pump; CCl_4, carbon tetrachloride; CL_{tot}, total clearance; CMZ, cefmetazole; K, elimination rate constant; Mdr, multidrug resistance; Mrp, multidrug resistance associated protein; MRT, mean residence time; Ntcp, Na^+-taurocholate co-transporting polypeptide; Oat, organic anion transporter; Oatp, organic anion transporting polypeptide; Oct, organic cation transporter; PCR, polymerase chain reaction; RT, reverse transcription; SLC, solute carrier; VRT, variance of residence time; V, volume of distribution

0006-2952/$ – see front matter © 2007 Published by Elsevier Inc.
doi:10.1016/j.bcp.2007.04.025

profile can be affected depending on the severity of liver dysfunction.

Carbon tetrachloride (CCl_4) is a well-known hepatotoxicant and has been frequently used for generating a liver-injured models of rat [2–4]. CCl_4 is bioactivated into trichloromethyl free radical by cytochrome P450 2E1 and trichloromethyl may be a cause of liver damage [5]. The liver dysfunction can be assessed by the aspartate aminotransferase (AST) and alanine aminotransferase (ALT) concentrations in serum. Therefore, in the present study, the relationship between the AST or ALT levels and urinary or fecal excretion was investigated in rats with CCl_4-induced liver dysfunction. We selected a cefamycin antibiotic, cefmetazole (CMZ), as a probe drug because CMZ has been reported to be excreted as an unchanged form in feces in rat [6].

Recently, hepatic transporters have been recognized as a major determinant of drug excretion and disposition [7–9]. There are many uptake or efflux transporters in the hepatic canalicular and sinusoidal membrane. Liver dysfunction has been reported to affect the expressions of some drug transporters [10]. Clarification of changes in the hepatic drug transporters could facilitate understanding the excretory profile in liver dysfunction. In the present study, we also performed DNA microarray analysis to evaluate the changes in the hepatic drug transporters by CCl_4-induced liver dysfunction in rat.

2. Materials and methods

2.1. Chemicals

CMZ and cefazolin were purchased from Sigma–Aldrich (St. Louis, MO). CCl_4, Transaminase CII-test Wako, and Creatinine-test Wako were purchased from Wako Pure Chemical Industries (Osaka, Japan). All primers shown in Table 1 were commercially synthesized at Hokkaido System Science (Sapporo, Japan). All other chemicals and solvents were of the highest or analytical grade commercially available.

Table 1 – Sequence of primers of rat transporter used in the present study

Primer	Sequence
Mdr1a S[a]	5′-ATCAACTCGCAAAAGCATCC-3′
Mdr1a AS[a]	5′-AATTCAACTTCAGGATCCGC-3′
Mdr1b S[a]	5′-CACTGGTGCCTCTGAGTTGA-3′
Mdr1b AS[a]	5′-GCACATCTTCATCCACATCCT-3′
Mrp2 S	5′-CAGTCACGGCTTCCTTTCTG-3′
Mrp2 AS	5′-AGGTTTCCGCTGGGACTTCT-3′
Mrp4 S[b]	5′-GACAGTTAGTGTGCCTTGCG-3′
Mrp4 AS[b]	5′-TGGTGAGAACAGTGCACTGG-3′
Bsep S	5′-TTACTCCGGAGAATAATGAG-3′
Bsep AS	5′-AGGGCTGACAGCAAGAATCA-3′
Oat2 S	5′-AATACTTGCTGAGCTGTGCC -3′
Oat2 AS	5′-AAACAGCAGCTGTGTCTGGT -3′

S, sense primer; AS, antisense primer.
[a] From Theron et al. [12].
[b] From Berezowski et al. [13].

2.2. CCl_4-induced liver dysfunction in rat

The present study was approved by the Institutional Animal Care and Use Committee of Kanazawa University. Male Sprague–Dawley rats (8 weeks old, SLC Japan, Hamamatsu, Japan) were intraperitoneally injected with CCl_4 at a dose of 640 mg/kg (a volume of 2 ml/kg) or corn oil once every 2 days for 45 days. The degree of liver dysfunction was assessed by the serum levels of AST and ALT measured. In addition, renal function was evaluated by the serum creatinine levels.

2.3. Excretion and pharmacokinetic of CMZ in CCl_4-treated rat

For the excretion study, CCl_4- or vehicle-treated rats were intravenously injected with CMZ at a dose of 100 mg/ml/kg at 24 h after the final CCl_4 treatment. Urine and feces samples were collected using metabolic cages for 24 h after the administration of CMZ. Before the CMZ treatment, blood samples were collected to measure AST, ALT, and creatinine levels.

For the pharmacokinetics study, CCl_4- or vehicle-treated rats were intravenously injected at a dose of 100 mg/ml/kg with CMZ at 24 h after the final CCl_4 treatment. Blood samples (0.2 ml) were collected at 0, 15, 30, 45, 60, 90, 120, and 180 min after the CMZ treatment.

2.4. Effect of CCl_4 discontinuation toward CMZ excretion

In four CCl_4-treated rats, the CCl_4 treatment was discontinued for 14 days after the 45 day CCl_4 treatment. After discontinuation, CCl_4-discontinued rats were injected with CMZ at a dose of 100 mg/ml/kg. Urine and feces samples were collected for 24 h.

2.5. Quantification of CMZ

The CMZ concentrations in urine, feces, and serum were quantified using high-performance liquid chromatography (HPLC) according to a method described previously with slight modifications [11]. Urine samples (0.1 ml) were diluted with 0.4 ml of distilled water. Feces samples were homogenized with distilled water and centrifuged at 1500 × *g* for 10 min. Serum samples (40 μl) were diluted with 20 μl of distilled water. The diluted urine, the supernatant of the feces, and the diluted serum were treated with 0.5% trichloroacetic acid in methanol containing cefazolin as an internal standard. After incubation at −20 °C for 20 min, the mixture was centrifuged at 15,000 × *g* for 10 min. Then the supernatant was diluted 1:1 with 0.1 M citrate buffer (pH 5.4). Fifty microliters aliquots of the sample were injected into the HPLC with a C_{30}-5 μm analytical column (Develosil, 4.6 mm × 150 mm, Nomura Chemical, Aichi, Japan). The mobile phase was methanol:10 mM citrate buffer (pH 5.4) = 13:87 (v/v) for the urine and feces samples or 20:80 (v/v) for the serum samples. The flow rate was 1.2 ml/min. The column temperature was 35 °C. The eluent was monitored at 254 nm.

2.6. Pharmacokinetic analysis

The pharmacokinetic parameters for CMZ were estimated from the serum concentration–time data by a moment

analysis. The area under the serum concentration curve from 0.25 to 3 h (AUC) was obtained using the trapezoidal rule. Statistical analyses were performed with GraphPad Instat computer program (GraphPad Software, San Diego, CA) by Student t-test.

2.7. RNA isolation

Total hepatic RNA was extracted using ISOGEN (Nippon Gene, Tokyo, Japan). Samples were divided into three groups based on the degree of liver dysfunction as follows: control group (AST <50 IU/l; ALT <25 IU/l), mild group (AST 50–600 IU/l; ALT 25–200 IU/l), and severe group (AST >600 IU/l; ALT >200 IU/l). Rats in the control group were treated with corn oil, while rats in the mild and severe groups were treated with CCl_4 once every 2 days for 45 days. Equal amounts of total mRNA from three rats in each group were pooled and used for microarray and real-time reverse transcription (RT)-polymerase chain reaction (PCR) analysis.

2.8. In vitro amplification and DNA microarray

In vitro amplification and DNA microarray analysis were performed using CodeLink™ Bioarray Perfect System according to the manufacturer's protocol (GE Healthcare Bioscience, Piscataway, NJ). cDNA was synthesized from pooled total RNA (2 μg) by RT reaction. The cDNA was used for in vitro transcription reaction by using biotine-11-UTP (Perkin-Elmer, Wellesley, MA). The labeled cRNA (10 μg) was applied to the DNA microarray (rat whole genome bioarray, GE Healthcare Bioscience). Hybridization was performed at 37 °C for 18 h. After washing, the microarray was stained by streptavidin-Cy 5 (Amersham Bioscience) and scanned in an Agilent G2565BA Microarray Scanner using Agilent Scan Control Software (Agilent Technologies, Palo Alto, CA). The image was analyzed using CodeLink™ Expression Analysis Software (GE Healthcare Bioscience).

2.9. Real-time RT-PCR

Hepatic drug transporters (Mdr1a, Mdr1b, Bsep, Mrp2, Mrp4, and Oat2) in rat were quantified by real-time RT-PCR. The sequences of the primers are shown in Table 1. cDNA was synthesized as described previously [14]. PCR was performed using the Smart Cycler (Cepheid, Sunnyvale, CA). The PCR conditions were as follows. After initial denaturing at 95 °C for 30 s, amplification was performed by denaturing at 94 °C for 4 s, and annealing and extension at 64 °C for 20 s for 45 cycles. Amplified products were monitored directly by measuring the increase of the dye intensity of SYBR Green I (Molecular Probes, Eugene, OR) that binds to double-strand DNA amplified by PCR.

3. Result

3.1. CCl_4-induced liver dysfunction in rat

In CCl_4-treated rats ($n = 18$), AST ranged from 91 to 3913 IU/l and ALT ranged from 37 to 1200 IU/l at 24 h after the final CCl_4 treatment. In control rats ($n = 5$), AST ranged from 26 to 37 IU/l and ALT ranged from 13 to 18 IU/l. The function of kidney was assessed by the creatinine concentrations in serum. There was no statistically significant difference in the serum creatinine concentration between the CCl_4-treated (0.89 ± 0.22 mg/dl) and control rats (0.86 ± 0.20 mg/dl). For the following experiments, these rats were divided into three groups as follows: control group ($n = 5$; AST <50 IU/l; ALT <25 IU/l); mild group ($n = 8$; AST 50–600 IU/l; ALT 25–200 IU/l); severe group ($n = 11$; AST >600 IU/l; ALT >200 IU/l).

3.2. CMZ excretion in CCl_4-treated rat

The relationship between the 24 h-cumulative urinary and fecal excretions of CMZ and the serum levels of AST or ALT are shown in Fig. 1. The excretion was calculated as the percentage of the total CMZ recovery. Fecal excretion was dominant in the control group. In CCl_4-treated rat, urinary excretion of CMZ increased, whereas the fecal excretion of CMZ decreased according to the increase of the AST and ALT levels. In CCl_4-treated rats, urinary excretion reached a plateau above 600 IU/l of AST or 200 IU/l of the ALT. The slopes of the fitted curves of the urinary and fecal excretions were different between rats with mild and those with severe liver dysfunction. The means of the urinary and fecal excretions, AST, and ALT was summarized in Table 2.

3.3. Pharmacokinetics of CMZ in CCl_4-treated rat

The serum concentrations of CMZ (Fig. 2) and the pharmacokinetic parameters (Table 3) in CCl_4-treated and control rats are shown. The serum concentrations of CMZ in the severe group were higher at all time points than those in the mild and control groups. On the other hand, the serum concentrations of CMZ in the mild group were similar to those in the control group. The AUC value of the severe group was significantly higher than that of the control group ($P < 0.05$). Other pharmacokinetic parameters of the mild and severe groups were not changed statistically, but the CL_{tot} and V values tended to be decreased by liver dysfunction.

3.4. Effect of CCl_4 discontinuation toward CMZ excretion

Fig. 3 shows the urinary and fecal CMZ excretions in the control, severe (before the CCl_4-discontinuation), and the discontinued rats. In the CCl_4-discontinued rats, urinary CMZ excretion was decreased while fecal CMZ excretion was increased as compared with severe rats. The excretory pattern of CMZ tended to recover by the CCl_4 discontinuation. The AST and ALT levels of CCl_4-discontinued rats (35.3 ± 3.3 and 16.8 ± 2.9 IU/l, respectively) became similar to those of control rats (31.1 ± 4.6 and 16.1 ± 2.1 IU/l, respectively).

3.5. Changes of hepatic mRNA expression by liver dysfunction

For the DNA microarray analysis, total RNA was pooled from the livers of three rats in the three groups (control, mild, and severe groups). The mean AST levels were 42.1, 468.7, and 1488.0 IU/l in the control, mild, and severe groups, respectively. Analyses of

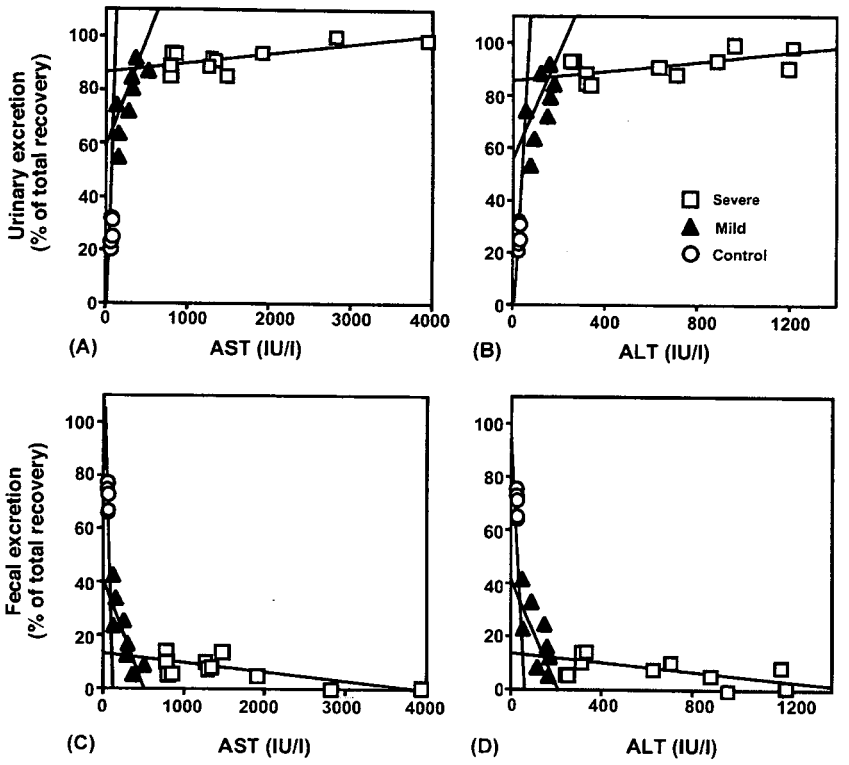

Fig. 1 – AST and ALT dependent-changes of urinary (A and B) and fecal (C and D) excretion of CMZ in individual rats with CCl_4-induced liver dysfunction. Control (○, $n = 5$), AST <50 IU/l, ALT <25 IU/l; mild (▲, $n = 8$), AST 50–600 IU/l, ALT 25–200 IU/l; severe (□, $n = 11$), AST >600 IU/l, ALT >200 IU/l.

the gene expression profiles identified that 1513 (980 up-regulated and 533 down-regulated) of 11,198 genes were commonly changed above 2-fold in the mild and severe groups. Especially, 8 (5 up-regulated and 3 down-regulated) of 30 genes of the ATP-binding cassette (ABC) transporters and 19 (10 up-regulated and 9 down-regulated) of 141 genes of the solute carrier (SLC) transporters were changed above 2-fold (Table 4). The expression changes of major hepatic drug transporters by the CCl_4 treatment are shown in Fig. 4. The expressions of all basolateral SLC transporters were decreased, whereas the expressions of basolateral ABC transporters except Mrp6 were increased depending on the AST levels. In the case of canalicular ABC transporters, the expression of Bsep and Mrp2 were decreased, but those of Mdr1a and Mdr1b were increased by the CCl_4 treatment. There was no change in Bcrp expression. To confirm the gene expression profiles of the DNA microarray shown in Fig. 4, real-time RT-PCR was performed in Mdr1a, Mdr1b, Bsep, Mrp2, Mrp4, and Oat2 genes (Fig. 5). The results of the expression profiles of six genes by real-time RT-PCR were almost the same as those by DNA microarray.

4. Discussion

In patients with liver disease, reductions in the doses of drugs are sometimes needed in clinical practice [15]. For the optimization of drug treatment, we should pay attention to changes in the pharmacokinetics in liver disease. It is

Table 2 – Excretion of CMZ and serum levels of AST and ALT in CCl_4-treated rat

	Control	CCl_4-treated	
		Mild	Severe
Urinary excretion (% of total recovery)	27.6 ± 5.1	77.8 ± 12.7**	92.3 ± 5.1***
Fecal excretion (% of total recovery)	72.4 ± 5.1	22.2 ± 12.7**	7.7 ± 5.1***
AST (IU/l)	31.1 ± 4.6	220.0 ± 130.3**	1551.2 ± 987.4***
ALT (IU/l)	16.1 ± 2.1	104.1 ± 48.1**	633.7 ± 368.8***

Data represent the mean ± S.D. (control, $n = 5$; mild, $n = 8$; severe, $n = 11$).
** $P < 0.01$ compared with control rat.
*** $P < 0.001$ compared with control rat.

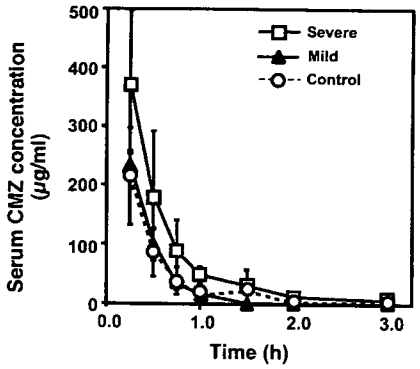

Fig. 2 – Serum concentration of CMZ in rats with CCl_4-induced liver dysfunction. Control (○), AST <50 IU/l, ALT <25 IU/l; mild (▲), AST 50–600 IU/l, ALT 25–200 IU/l; severe (□), AST >600 IU/l, ALT >200 IU/l. Data represent the mean ± S.D. (control, $n = 5$; mild, $n = 3$; severe, $n = 3$).

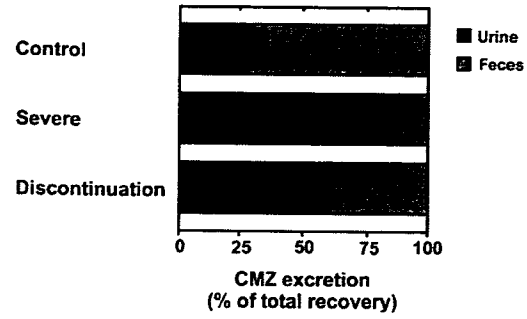

Fig. 3 – Changes of CMZ excretion after 14-day discontinuation of CCl_4 treatment. Control, corn oil treatment once every 2 days for 45 days; severe, CCl_4 treatment once every 2 days for 45 days and then showing severe liver dysfunction; discontinuation, non-treatment for 2 weeks after 45-day CCl_4 treatment. Data represent the mean ± S.D. (control, $n = 5$; CCl_4, $n = 4$; discontinuation, $n = 4$).

important to predict hepatic function such as biliary excretion. In the present study, we first investigated the relationship between liver dysfunction and the excretory pathway of a drug.

In the present study, liver dysfunction was induced by treatment with a typical hepatotoxicant, CCl_4, in rat. Since there were no statistical differences in the serum creatinine concentrations between CCl_4-treated and control rats, there appeared to be no renal dysfunction in the present study. In spite of the same experimental condition, liver dysfunction with various AST and ALT levels was generated by CCl_4 treatment in the rats. This may be due to differences in the interindividual sensitivity of CCl_4, but the reason is still unclear. A large interindividual variability of CCl_4-induced cytotoxicity in a histological study of rat livers has been reported [16].

CMZ is predominantly eliminated by the biliary route under normal conditions in rat [6]. In the present study, the urinary excretion was increased and the fecal excretion was decreased by CCl_4-induced liver dysfunction. The excretion pathway of CMZ was changed prominently in the range from 50 to 600 IU/l of AST and from 25 to 200 IU/l of ALT, indicating that the excretion of CMZ might be changed in response to an increase in the AST and ALT levels. Urinary excretion of bile acid and drugs is increased by liver disease [17–19], which is assumed to be a type of detoxification. Therefore, a change of the CMZ excretory pathway might also result in detoxification. After 14-day discontinuation of CCl_4 treatment, CMZ excretion tended to return to the normal excretory pattern, resembling that in

Table 3 – Pharmacokinetic parameters of CMZ in CCl_4-treated rat

	Control	CCl_4-treated	
		Mild	Severe
AUC (mg h/l)	106.6 ± 38.9	100.7 ± 10.2	210.1 ± 68.5*
MRT (h)	0.6 ± 0.3	0.4 ± 0.1	0.7 ± 0.2
VRT	0.9 ± 0.2	0.6 ± 0.3	0.5 ± 0.2
CL_{tot} (l/h)	0.5 ± 0.2	0.4 ± 0.0	0.2 ± 0.1
K (h^{-1})	1.8 ± 0.7	2.5 ± 0.0	1.5 ± 0.4
V (l)	0.3 ± 0.1	0.2 ± 0.0	0.1 ± 0.1

Data represent the mean ± S.D. (control, $n = 5$; mild, $n = 3$; severe, $n = 3$). AUC, area under the serum concentration–time curve; MRT, mean residence time; VRT, variance of residence time; CL_{tot}, total clearance; K, elimination rate constant; V, volume of distribution.
* $P < 0.05$ compared with control rat.

Table 4 – Expression changes of hepatic transporters in both mild and severe groups

Common name	GeneBank ID	Fold induction	
		Mild	Severe
Up regulation			
Mdr1a	NM_133401	4.73	8.66
Mdr1b	NM_012623	10.18	21.50
Mrp1	NM_022281	3.68	3.48
Mrp4	AW141985	3.64	3.27
Abcg1	NM_053502	2.46	3.33
Glast	NM_019225	7.56	3.24
Cat-1	NM_013111	7.23	17.46
Mct7b	BQ200772	3.82	3.47
Pit-1	NM_031148	2.97	3.72
Ant1	NM_053515	5.07	4.44
Slc35b2	NM_199111	2.11	2.33
Slc39a1	NM_133315	2.01	2.06
Down regulation			
Mrp2	NM_012833	0.40	0.35
Mrp6	NM_031013	0.41	0.20
Sur	NM_013039	0.29	0.18
Slc2a5	NM_031741	0.32	0.19
Slc6a6	NM_017206	0.41	0.33
Gat2	NM_133623	0.40	0.22
Nadc1	NM_031746	0.32	0.18
Tat1	NM_138831	0.41	0.46
Oct	NM_012697	0.46	0.28
Oat3	NM_031332	0.33	0.10
Nckx3	AY009158	0.32	0.21
NaPi-Iib	NM_053380	0.47	0.32

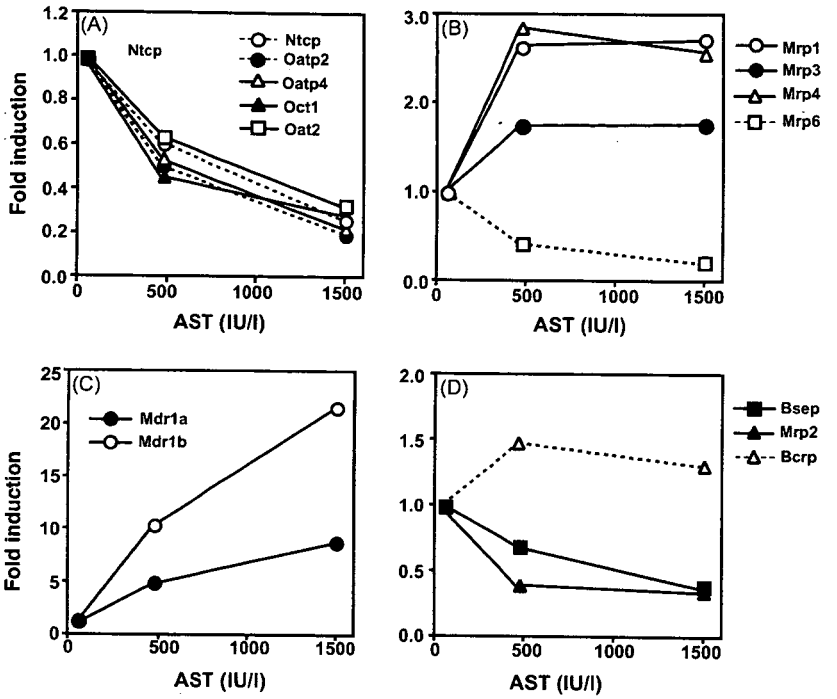

Fig. 4 – Expression profile of hepatic transporters measured by DNA microarray. (A) Basolateral SLC transporters; (B) basolateral ABC transporters; (C) canalicular Mdr1 transporters; (D) canalicular ABC transporters except Mdr1.

the control rats. Although the AST and ALT levels were normal in CCl_4-discontinued rats, the rate of urinary and fecal excretion was similar but not the same as in the control rats. The AST or ALT levels may be clearly corresponded with changes of the excretion pathway during exacerbation but not during convalescence of the liver dysfunction. Lopez et al. [20] reported that biliary CMZ excretion decreased in cirrhosis rat, but they did not investigate in detail.

Some factors including molecular weight, lipophilicity, and protein-binding rate have been reported to be involved in determining the excretory pathway and rate [21,22]. Recently, hepatic transports have been recognized as an important determinant of the drug disposition. Actually, biliary clearance of a typical P-gp substrate, digoxin, was decreased by administration of a P-gp inhibitor, quinidine, in healthy volunteers [23]. Biliary excretion clearance of the Bcrp substrate, pitavastatin, was decreased in Bcrp knockout mice [24]. It still remains unclear whether CMZ can be transported by an active carrier system. Therefore, DNA microarray was performed to evaluate the changes in the expression of various hepatic transporters by CCl_4-induced liver dysfunction in the present study. The expressions of many hepatic transporters were changed by the CCl_4 treatment (Table 4). An altered expression of transporters may influence the drug disposition and excretion. In terms of the genes shown in Fig. 4, the changes in expression may depend on the severity of liver dysfunction. The administration of CCl_4 resulted in reduced expression of basolateral SLC transporter genes and induced the expression of basolateral ABC transporter genes (Fig. 4). Ntcp (Slc10a1) and Oatp2 (Slc21a5) are uptake transporters in the liver and were reported to be decreased in acute liver dysfunction induced by CCl_4 in rat [25]. In the case of canalicular ABC transporters, the expression of Mdr1a and Mdr1b genes was up-regulated, whereas that of Bsep and Mrp2 genes was down-regulated by the CCl_4 treatment in the present study. It was reporter that Mdr1 was increased and

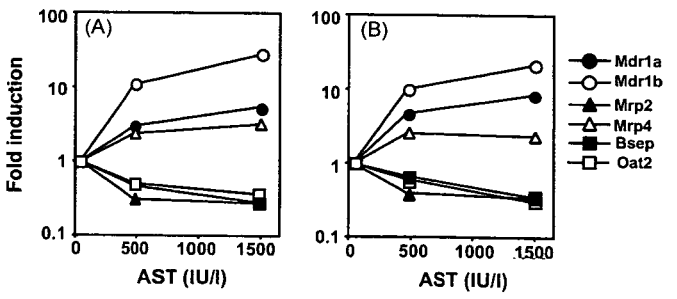

Fig. 5 – Comparison of expression profile of hepatic transporters between real-time RT-PCR (A) and DNA microarray (B).

Mrp2 was decreased by a single CCl_4 treatment in rat [26,27], which corresponded with our results. Moreover, it was reported that the expression of hepatic Mrp1 and Mrp4 was up-regulated, whereas that of hepatic Ntcp was down-regulated in mice by a single CCl_4 treatment [28,29]. Taking the results of the present study and those of previous reports into consideration, alterations in the gene expression of drug transporters may lead to decreased uptake into hepatocytes and increased efflux from hepatocytes. Aleksunes et al. [28,29] suggested that the induction of efflux transporters might be coordinated with the reduction of uptake transporters and this phenomenon would be a defense mechanism for rapid elimination of xenobiotics. Cherrington et al. [30] also indicated that alterations in transporter expression might be related to hepatoprotection, representing a regulation for compensatory process. Our present results would support their hypotheses.

It is still unknown whether CMZ can be transported via drug transporters in the liver, although some cephalosporin antibiotics could be transported by Oat family transporters (Slc22a) [31,32]. In the preliminary study, it was clarified that CMZ was not a substrate for human P-gp, human MRP2, rat Bsep, and rat Bcrp by the measurement of the ATPase activity using the membrane fraction from baculovirus-infected insect cells expressing human P-gp, human MRP2, rat Bsep, or rat Bcrp, respectively (data not shown). Taking the present results into consideration, Mrp4 and/or Mrp3 might be involved in CMZ transport, but further study is needed to clarify the mechanism of CMZ elimination. The increase in urinary excretion and the decrease in biliary excretion of CMZ would be caused by changes in the expression of drug transporters.

In conclusion, liver dysfunction affected the urinary and fecal CMZ excretion in rat in AST- and ALT-dependent manners. This phenomenon could be partly explained by the changes in the expression of drug transporters in liver dysfunction. The present study could provide useful information for the prediction of pharmacokinetics in liver dysfunction.

Acknowledgments

This work was supported in part by Research on Advanced Medical Technology, Health and Labor Science Research Grants from the Ministry of Health, Labor and Welfare of Japan. We thank Mr. Brent Bell for reviewing the manuscript.

REFERENCES

[1] Greenfield RA, Gerber AU, Craig WA. Pharmacokinetics of cefoperazone in patients with normal and impaired hepatic and renal function. Rev Infect Dis 1983;5:S127–36.
[2] Park EJ, Jeon CH, Ko G, Kim J, Sohn DH. Protective effect of curcumin in rat liver injury induced by carbon tetrachloride. J Pharm Pharmacol 2000;52:437–40.
[3] Yokogawa K, Watanabe M, Takeshita H, Nomura M, Mano Y, Miyamoto K. Serum aminotransferase activity as a predictor of clearance of drugs metabolized by CYP isoforms in rats with acute hepatic failure induced by carbon tetrachloride. Int J Pharm 2004;269:479–89.
[4] Minami K, Saito T, Narahara M, Tomita H, Kato H, Sugiyama H, et al. Relationship between hepatic gene expression profiles and hepatotoxicity in five typical hepatotoxicant-administered rats. Toxicol Sci 2005;87:296–305.
[5] Jeong HG. Inhibition of cytochrome P450 2E1 expression by oleanolic acid: hepatoprotective effects against carbon tetrachloride-induced hepatic injury. Toxicol Lett 1999;105:215–22.
[6] Murakawa T, Sakamoto H, Fukada S, Nakamoto S, Hirose T, Itoh N, et al. Pharmacokinetics of ceftizoxime in animals after parenteral dosing. Antimicrob Agents Chemother 1980;17:157–64.
[7] Faber KN, Muller M, Jansen PL. Drug transport proteins in the liver. Adv Drug Deliv Rev 2003;55:107–24.
[8] Chandra P, Brouwer KL. The complexities of hepatic drug transport: current knowledge and emerging concepts. Pharm Res 2004;21:719–35.
[9] Shitara Y, Sato H, Sugiyama Y. Evaluation of drug-drug interaction in the hepatobiliary and renal transport of drugs. Annu Rev Pharmacol Toxicol 2005;45:689–723.
[10] Trauner M, Boyer JL. Bile salt transporters: molecular characterization, function, and regulation. Physiol Rev 2003;83:633–71.
[11] Welage LS, Borin MT, Wilton JH, Hejmanowski LG, Wels PB, Schentag JJ. Comparative evaluation of the pharmacokinetics of *N*-methylthiotetrazole following administration of cefoperazone, cefotetan, and cefmetazole. Antimicrob Agents Chemother 1990;34:2369–74.
[12] Theron D, Barraud de Lagerie S, Tardivel S, Pelerin H, Demeuse P, Mercier C, et al. Influence of tumor necrosis factor-alpha on the expression and function of P-glycoprotein in an immortalised rat brain capillary endothelial cell line GPNT. Biochem Pharmacol 2003;66:579–87.
[13] Berezowski V, Landry C, Dehouck MP, Cecchelli R, Fenart L. Contribution of glial cells and pericytes to the mRNA profiles of P-glycoprotein and multidrug resistance-associated proteins in an in vitro model of the blood-brain barrier. Brain Res 2004;1018:1–9.
[14] Iwanari M, Nakajima M, Kizu R, Hayakawa K, Yokoi T. Induction of CYP1A1, CYP1A2, and CYP1B1 mRNAs by nitropolycyclic aromatic hydrocarbons in various human tissue-derived cells: chemical-, cytochrome P450 isoform-, and cell-specific differences. Arch Toxicol 2002;76:287–98.
[15] McLean AJ, Morgan DJ. Clinical pharmacokinetics in patients with liver disease. Clin Pharmacokinet 1991;21: 42–69.
[16] Cikrt M, Tichy M, Holusa R. Biliary excretion of 64Cu 65Zn and 203Hg in the rat with liver injury induced by CCl_4. Arch Toxicol 1975;34:227–36.
[17] Makino I, Hashimoto H, Shinozaki K, Yoshino K, Nakagawa S. Sulfated and nonsulfated bile acids in urine, serum, and bile of patients with hepatobiliary diseases. Gastroenterology 1975;68:545–53.
[18] Cochet B, Belaieff J, Allaz AF, Rudhardt M, Balant L, Fabre J. Decreased extrarenal clearance of cefoperazone in hepatocellular diseases. Br J Clin Pharmacol 1981;11:389–90.
[19] Boscia JA, Korzeniowski OM, Snepar R, Kobasa WD, Levison ME, Kaye D. Cefoperazone pharmacokinetics in normal subjects and patients with cirrhosis. Antimicrob Agents Chemother 1983;23:385–9.
[20] Lopez P, Garcia-Pardo LA, Gonzalez-Gallego J, Gonzalez P, Tunon MJ. Alterations induced by fascioliasis and cirrhosis on the biliary excretion of cefmetazole in Wistar rats. Comp Biochem Physiol C 1992;103:53–6.
[21] Hirom PC, Millburn P, Smith RL, Williams RT. Species variations in the threshold molecular-weight factor for the biliary excretion of organic anions. Biochem J 1972;129:1071–7.

[22] Fleck C, Braunlich H. Factors determining the relationship between renal and hepatic excretion of xenobiotics. Arzneimittelforschung 1990;40:942–6.
[23] Angelin B, Arvidsson A, Dahlqvist R, Hedman A, Schenck-Gustafsson K. Quinidine reduces biliary clearance of digoxin in man. Eur J Clin Invest 1987;17:262–5.
[24] Hirano M, Maeda K, Matsushima S, Nozaki Y, Kusuhara H, Sugiyama Y. Involvement of BCRP (ABCG2) in the biliary excretion of pitavastatin. Mol Pharmacol 2005;68:800–7.
[25] Geier A, Dietrich CG, Voigt S, Kim SK, Gerloff T, Kullak-Ublick GA, et al. Effects of proinflammatory cytokines on rat organic anion transporters during toxic liver injury and cholestasis. Hepatology 2003;38:345–54.
[26] Kier LD, Neft R, Tang L, Suizu R, Cook T, Onsurez K, et al. Applications of microarrays with toxicologically relevant genes (tox genes) for the evaluation of chemical toxicants in Sprague Dawley rats in vivo and human hepatocytes in vitro. Mutat Res 2004;549:101–13.
[27] Song IS, Lee YM, Chung SJ, Shim CK. Multiple alterations of canalicular membrane transport activities in rats with CCl_4-induced hepatic injury. Drug Metab Dispos 2003;31:482–90.
[28] Aleksunes LM, Scheffer GL, Jakowski AB, Pruimboom-Brees IM, Manautou JE. Coordinated expression of multidrug resistance-associated proteins (Mrps) in mouse liver during toxicant-induced injury. Toxicol Sci 2006;89:370–9.
[29] Aleksunes LM, Slitt AM, Cherrington NJ, Thibodeau MS, Klaassen CD, Manautou JE. Differential expression of mouse hepatic transporter genes in response to acetaminophen and carbon tetrachloride. Toxicol Sci 2005;83:44–52.
[30] Cherrington NJ, Slitt AL, Li N, Klaassen CD. Lipopolysaccharide-mediated regulation of hepatic transporter mRNA levels in rats. Drug Metab Dispos 2004;32:734–41.
[31] Uwai Y, Saito H, Inui K. Rat renal organic anion transporter rOAT1 mediates transport of urinary-excreted cephalosporins, but not of biliary-excreted cefoperazone. Drug Metab Pharmacokinet 2002;17:125–9.
[32] Khamdang S, Takeda M, Babu E, Noshiro R, Onozato ML, Tojo A, et al. Interaction of human and rat organic anion transporter 2 with various cephalosporin antibiotics. Eur J Pharmacol 2003;465:1–7.

0090-9556/07/3509-1642–1648$20.00
DRUG METABOLISM AND DISPOSITION
Copyright © 2007 by The American Society for Pharmacology and Experimental Therapeutics
DMD 35:1642–1648, 2007

Vol. 35, No. 9
16097/3247781
Printed in U.S.A.

Glucuronidation of Thyroxine in Human Liver, Jejunum, and Kidney Microsomes

Hiroyuki Yamanaka, Miki Nakajima, Miki Katoh, and Tsuyoshi Yokoi

Drug Metabolism and Toxicology, Division of Pharmaceutical Sciences, Graduate School of Medical Science, Kanazawa University, Kanazawa, Japan

Received April 3, 2007; accepted June 19, 2007

ABSTRACT:

Glucuronidation of thyroxine is a major metabolic pathway facilitating its excretion. In this study, we characterized the glucuronidation of thyroxine in human liver, jejunum, and kidney microsomes, and identified human UDP-glucuronosyltransferase (UGT) isoforms involved in the activity. Human jejunum microsomes showed a lower K_m value (24.2 μM) than human liver (85.9 μM) and kidney (53.3 μM) microsomes did. Human kidney microsomes showed a lower V_{max} value (22.6 pmol/min/mg) than human liver (133.4 pmol/min/mg) and jejunum (184.6 pmol/min/mg) microsomes did. By scaling-up, the in vivo clearances in liver, intestine, and kidney were estimated to be 1440, 702, and 79 μl/min/kg body weight, respectively. Recombinant human UGT1A8 (108.7 pmol/min/unit), UGT1A3 (91.6 pmol/min/unit), and UGT1A10 (47.3 pmol/min/unit) showed high, and UGT1A1 (26.0 pmol/min/unit) showed moderate thyroxine glucuronosyltransferase activity. The thyroxine glucuronosyltransferase activity in microsomes from 12 human livers was significantly correlated with bilirubin *O*-glucuronosyltransferase ($r = 0.855$, $p < 0.001$) and estradiol 3-*O*-glucuronosyltransferase ($r = 0.827$, $p < 0.0001$) activities catalyzed by UGT1A1, indicating that the activity in human liver is mainly catalyzed by UGT1A1. Kinetic and inhibition analyses suggested that the thyroxine glucuronidation in human jejunum microsomes was mainly catalyzed by UGT1A8 and UGT1A10 and to a lesser extent by UGT1A1, and the activity in human kidney microsomes was mainly catalyzed by UGT1A7, UGT1A9, and UGT1A10. The changes of activities of these UGT1A isoforms via inhibition and induction by administered drugs as well as genetic polymorphisms may be a causal factor of interindividual differences in the plasma thyroxine concentration.

Thyroid hormones mediate many physiological processes including embryonic development, cellular differentiation, metabolism, and the regulation of cell proliferation (Hulbert, 2000; Wu and Koenig, 2000; Zhang and Lazar, 2000). The plasma concentrations of thyroid hormones are strictly controlled by thyroid-stimulating hormone, which is subjected to negative feedback regulation by thyroid hormones. The major form of thyroid hormone secreted from thyroid gland is thyroxine. In hypothyroidism, thyroxine is orally administered to keep the plasma thyroid hormone level normal. Thyroxine has little biological activity and is converted to the active form, triiodothyronine (T3) mainly in human liver and kidney (Leonard and Koehrle, 1996). In human, approximately 80% of the total plasma T3 is produced by thyroxine via outer ring deiodination (Fig. 1). In addition to deiodination, thyroxine is metabolized to sulfate and glucuronide by sulfotransferases and UDP-glucuronosyltransferases (UGTs), respectively (Fig. 1). The thyroxine sulfate hardly appears in bile, urine, or serum, because it is rapidly degraded by inner ring deiodination in the liver. In contrast to the sulfate, thyroxine glucuronide is readily excreted into bile and subsequently hydrolyzed by β-glucuronidases in the intestine, and may affect the enterohepatic circulation of thyroxine (Visser, 1994). It has been reported that administration of UGT inducers such as phenytoin, carbamazepine (Isojarvi et al., 1992), and rifampicin (Ohnhaus and Studer, 1983) markedly decreased serum thyroxine levels in patients. Thus, glucuronidation is a major metabolic pathway to control the serum thyroxine level.

In humans, UGTs are divided into two families: UGT1 and UGT2 (Mackenzie et al., 2005). The *UGT1* and *UGT2* genes appear to be structurally different in that the UGT1 proteins result from alternate splicing of the unique first exon with four common exons encoded by the *UGT1* gene complex, whereas UGT2 proteins appear to be encoded by unique genes. In humans, there are nine functional UGT1A and seven UGT2B proteins (Mackenzie et al., 2005). Among them, human UGT1A1 and UGT1A9 have been reported to catalyze thyroxine glucuronidation (Findlay et al., 2000). However, a limitation of the study was that only two UGT isoforms were investigated. The first purpose of the present study is to investigate the catalytic activity of thyroxine glucuronidation by all human UGT isoforms for which recombinant proteins are currently available.

Human UGTs are expressed in a tissue-specific manner. Table 1 summarizes the UGT isoforms expressed in human liver, intestine, and kidney (King et al., 2000; Tukey and Strassburg, 2000; Fisher et al., 2001; Levesque et al., 2001; Basu et al., 2004, Finel et al., 2005). In general, liver plays an important role in the glucuronidation of most

H.Y. was supported as a Research Fellow of the Japan Society for the Promotion of Science.

Article, publication date, and citation information can be found at http://dmd.aspetjournals.org.

doi:10.1124/dmd.107.016097.

ABBREVIATIONS: T3, triiodothyronine; LC-MS/MS, liquid chromatography-mass/mass spectrometry; UGT, UDP-glucuronosyltransferase; UDPGA, UDP-glucuronic acid.

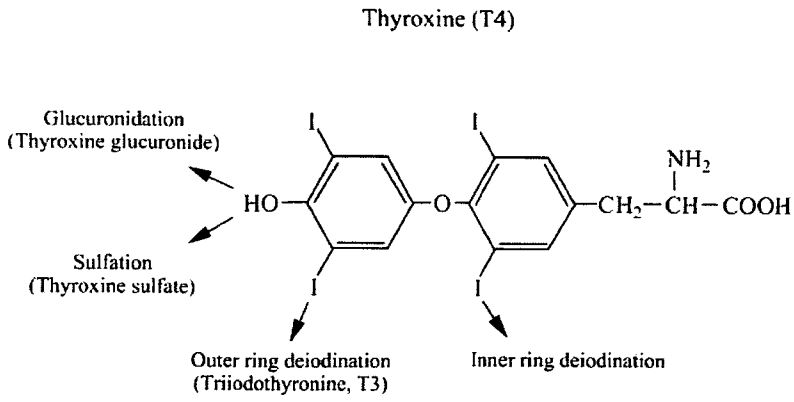

FIG. 1. Major metabolic pathways of thyroxine in human.

TABLE 1

Tissue distribution of human UGT mRNAs

Data are from King et al. (2000), Tukey and Strassburg (2000), Fisher et al. (2001), Levesque et al. (2001), Basu et al. (2004), and Finel et al. (2005).

Tissue	UGT Isoform															
	1A1	1A3	1A4	1A5	1A6	1A7	1A8	1A9	1A10	2B4	2B7	2B10	2B11	2B15	2B17	2B28
Liver	+	+	+	+	+	−	−	+	−	+	+	+	+	+	+	+
Intestine	+	+	+	+	+	−	+	−	+	+	+	+	−	+	−	+
Kidney	−	−	−	N.D.	+	+	−	+	+	+	+	+	+	+	+	+

N.D., no data: +, present; −, not detectable.

drugs, but extrahepatic tissues also contribute significantly to the glucuronidation of certain drugs in human (Krishna and Klotz, 1994). It is conceivable that the glucuronidation of thyroxine occurs not only in liver but also in intestine and kidney. The second purpose of the present study is to characterize thyroxine glucuronidation in human liver, jejunum, and kidney microsomes, and to identify the UGT isoforms involved in the glucuronidation in each tissue.

Materials and Methods

Materials. Thyroxine, UDP-glucuronic acid (UDPGA), and alamethicin were purchased from Sigma-Aldrich (St. Louis, MO). Bilirubin, chenodeoxycholic acid, serotonin, imipramine hydrochloride, and propofol were purchased from Wako Pure Chemicals (Osaka, Japan). Morphine hydrochloride was from Takeda Chemical Industries (Osaka, Japan). Pooled human liver microsomes (lot H161), microsomes from 12 individual human livers (H003, H023, H030, H043, H056, H064, H066, H070, H089, H093, H112, and HK23), recombinant human UGT1A1, UGT1A3, UGT1A4, UGT1A6, UGT1A7, UGT1A8, UGT1A9, UGT1A10, UGT2B4, UGT2B7, UGT2B15, and UGT2B17 expressed in baculovirus-infected insect cells (Supersomes), and UGT control Supersomes were purchased from BD Gentest (Woburn, MA). The human jejunum (lot HJM0023) or kidney (lot 045290170002) microsomes from an individual donor were purchased from KAC (Kyoto Japan). All other chemicals and solvents were of analytical or the highest grade commercially available.

Thyroxine Glucuronidation Assay. A typical incubation mixture (100 μl total volume) contained 100 mM Tris-HCl buffer (pH 7.4), 5 mM $MgCl_2$, 5 mM UDPGA, 25 μg/ml alamethicin, 0.4 mg/ml human liver, jejunum, or kidney microsomes or recombinant UGTs, and 50 μM thyroxine. Thyroxine was dissolved in dimethyl sulfoxide/0.05 M sodium hydroxide (50:50). The final concentration of the organic solvents in the incubation mixture was 1% (v/v). The reaction was initiated by the addition of UDPGA. After incubation at 37°C for 90 min, the reaction was terminated by adding 100 μl of ice-cold 94% acetnitrile/6% formic acid. After the centrifugation at 12,000 rpm for 5 min, the supernatant was filtered with a 0.22-μm filter (Ultrafree-MC centrifugal filter unit; Millipore, Eschborn, Germany). Aliquots of 10 μl were injected into the LC-MS/MS system.

LC-MS/MS Analysis for Thyroxine Glucuronides. LC was performed using an HP1100 system including a binary pump, an automatic sampler, and a column oven (Agilent Technologies, Waldbronn, Germany), which was equipped with a Mightysil RP-18 GP (4.6 × 150 mm; 5 μm) column (Kanto Chemical, Tokyo, Japan). The column temperature was 35°C. The mobile phase was 0.1% formic acid (A) and acetonitrile including 0.1% formic acid (B). The conditions for elution were as follows: 25% B (0–1 min); 25 to 70% B (1–4 min); 70% B (4–10 min); 70 to 25% B (10–11 min). Linear gradients were used for all solvent changes. The flow rate was 0.5 ml/min. The LC apparatus was connected to a PE Sciex API2000 tandem mass spectrometer (Applied Biosystems, Langen, Germany) operated in the positive electrospray ionization mode. The turbo gas was maintained at 450°C. Nitrogen was used as the nebulizing, turbo, and curtain gas at 50, 80, and 20 psi, respectively. Parent and/or fragment ions were filtered in the first quadrupole and dissociated in the collision cell using nitrogen as the collision gas. The collision energy was 20 V and 26 V for thyroxine and thyroxine glucuronides, respectively. Two mass/charge (m/z) ion transitions were recorded in the multiple reaction monitoring mode: m/z 778 and 778 for thyroxine, and m/z 954 and 778 for thyroxine glucuronide. The retention times of thyroxine glucuronide and thyroxine were 7.1 min and 8.9 min, respectively. For the quantification of thyroxine glucuronide, the eluate of the HPLC from the incubation mixture including thyroxine glucuronide was collected, referring to the retention time. A part of the eluate was incubated with 800 U/ml β-glucuronidase at 37°C for 24 h. The produced thyroxine was quantified by LC-MS/MS. Once we determined the peak area per known content of thyroxine glucuronide, the ratio was applied to the calculation of the thyroxine glucuronide formed in the incubation mixtures.

Kinetic Analyses of Thyroxine Glucuronidation in Human Liver, Jejunum, and Kidney Microsomes or Recombinant UGTs. Thyroxine glucuronosyltransferase activities were determined as described above with substrate concentrations from 2 μM to 100 μM. Kinetic parameters were estimated from the fitted curve using a computer program (KaleidaGraph; Synergy Software, Reading, PA) designed for nonlinear regression analysis. The following equations were applied for Michaelis-Menten kinetics (eq. 1) or substrate inhibition kinetics (eq. 2) (Houston and Kenworthy, 2000):

$$V = V_{max} \times S/(K_m + S) \quad (1)$$

$$V = V_{max} \times S/(K_m + S + S^2/K_{si}) \quad (2)$$

where V is the velocity of the reaction, S is the substrate concentration, K_m is Michaelis-Menten constant, V_{max} is the maximum velocity, and K_{si} is the